Paper No. 111

ISMS 2016

Numerical analysis of Westwood Mine tailings embankment stability during the restoration phase

Yaya Coulibaly*, Tikou Belem, Li Zhen Cheng

Research Institute on Mines and Environment (RIME)
Université du Québec en Abitibi-Témiscamingue (UQAT)
Tel: +1 819-874-8728 ext. 6233

ABSTRACT
Stability analysis of Westwood Mine tailings embankment performed using SLOPE/W and SIGMA/W codes showed that the minimum factor of safety obtained is higher than the recommended value of 1.5 set by some authors and the Quebec Ministry of Natural Resources and Wildlife for static loading and steady flow conditions. Pore pressures that must be controlled are higher in bottom layers of the embankment, and these pressures move toward the downstream side. In addition, low electrical resistivity values (by geophysical method) associated with the high water content tailings layer, suggest its susceptibility to internal erosion.

1. INTRODUCTION

The mining industry is the lung of the economy of any country possessing active mines, but it also generates large quantities of solid wastes such as tailings and waste rock that must be properly confined either in a tailings storage facility (TSF) or waste rock pile, respectively. The exposure of these solid wastes to atmospheric conditions could result in environmental pollution by acid mine drainage (AMD) or contaminated neutral drainage (CND). When underground mining methods require that the stopes are artificially supported to allow full ore recovery, backfilling is an effective way of solid wastes management. Mine tailings are surrounded in the TSF by embankments that must be monitored to prevent spillage of slurry tailings due to their potential failure. Failure is a physical process (mechanical or hydraulic) by which the embankment can be broken by tearing off and dumps potentially contaminated slurry tailings and, consequently, floods the downstream side of the dam. In general, breakdown of embankment dams is *via* four classical mechanisms (Mériaux et al., 2001): external erosion, internal erosion, external instability and liquefaction. Runoff of rainwater can also be the cause of external erosion. The settlement on the ridge causing cracking and water infiltration into the dam can cause internal erosion or slippage in an area of weakness.

Numerical analysis methods have been widely used to solve complex problems of slope stability, which otherwise would not be possible using conventional techniques (Eberhardt, 2003; Barbour and Krahn, 2004; Ormann et al., 2010; GEO-SLOPE International Ltd., 2007). Also, the geophysical method using electrical resistivity has excellent potential, as the measured parameters (resistivity or conductivity) are sensitive to the presence of water or cavities (Denahan and Smith, 1984; Ernstson and Kirsch, 2006). Among other things, electrical resistivity method makes it possible to detect the internal structure and cracks in the embankment.

Figure 1: Aerial view of the tailings embankment studied.

The Westwood Mine (owned by IAMGold Corp.) aims at reusing their TSF #1 for solid wastes storage, but on the other side of the Northwest separation embankment is located a small polishing pond (Figure 1). Some sporadic and localized slumps and slippage on the embankment have been reported. The slippage occurs on the downstream side slope (external instability) and the upstream slope side for some reason (e.g. liquefaction of the tailings or

*Corresponding author – email : yaya.coulibaly@uqat.ca

foundation soil as a result of a probable low magnitude seismic event).

The aim of this study is to assess the embankment stability by the means of numerical analysis using SLOPE/W and SIGMA/W codes (from GEO-SLOPE International Ltd.) and of geophysical methods that use electrical resistivity and ground-penetrating radar (GPR). The SLOPE/W code is based on limit-equilibrium analysis, while the SIGMA/W code is based on finite element method (FEM). The SLOPE/W code was used for assessing the embankment slope stability analysis through the calculation of the factor of safety (FS) based on the strength reduction factor (SRF) method. The SIGMA/W code was used for obtaining the stress and strain distribution across the embankment. The geophysical methods (electrical resistivity and GPR) show excellent potential of correlating all the data since the tailings dam properties (resistivity or conductivity) measured are sensitive to the presence of water or cavities. This paper presents the main results obtained.

2. METHODS OF SLOPE STABILITY ANALYSIS USING NUMERICAL CODES

2.1 Factor of safety (SLOPE/W)

In conventional methods of limit equilibrium analysis, the factor of safety (FS) is defined as the ratio between the resisting forces and the forces leading to tilting movements (Krahn, 2007, in GEO-SLOPE International Ltd., 2007).

$$\mathrm{FS} = \frac{\sum S_r}{\sum S_m} \quad (1)$$

where S_r = resisting force due to friction and cohesion; S_m = driving force tending to drag the block.

Alternatively, the factor of safety can also be expressed as follows:

$$\mathrm{FS} = \frac{Moments\ resisting\ sliding}{Moments\ causing\ sliding} \quad (2)$$

Amongst the most popular analytical methods of limit equilibrium analysis (see Figure 2), the Morgenstern-Price method was chosen as the analysis method (which is close to the Spencer's method), because it expresses two basic concepts for determining the factor of safety. The factor of safety versus lambda (Lamé coefficient) indicates the minimum factor of safety at the point of intersection of equilibrium moment and equilibrium force. From Figure 2 the point of intersection of the moment and the force corresponds to a factor of safety of 2.15, according to Morgenstern-Price or Spencer methods. In practice, the use of FS greater than 1.5 for static analysis of embankment stability and steady flow conditions is recommended (Eberhardt, 2003; Ormann et al., 2010; Quebec Ministry of Natural Resources and Wildlife).

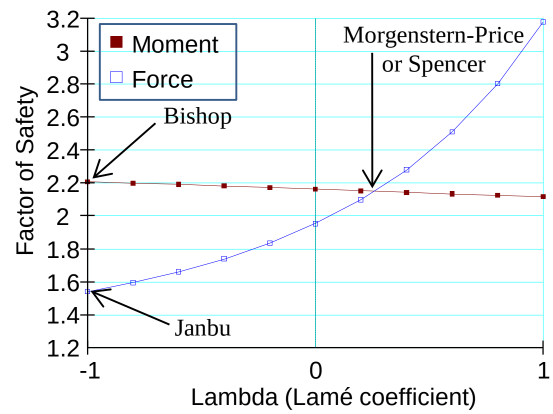

Figure 2: Graphical plot of the factor of safety as a function of Lamé coefficient for the moment and equilibrium force.

2.2 Stress-strain analysis (SIGMA/W)

The stress-strain analysis was performed by the finite element method using the SIGMA/W numerical code. The embankment slope stability was assessed by the effective stress analysis and the Mohr-Coulomb failure criterion was chosen:

$$\tau = c' + \sigma' tan\varphi' \quad (3)$$

where τ is the shear strength (kPa), c' is the effective cohesion (kPa), φ' is the effective internal friction angle (°) and σ' is the effective normal stress (kPa) which is given as follows:

$$\sigma' = \sigma - u \quad (4)$$

where u is the pore water pressure (kPa) and σ is the normal or vertical total stress (kPa).

The reduction of the effective stress σ' will reduce the shear resistance and this could promote some instabilities. For each simulation, the convergence of the calculations were be analyzed by the unbalanced forces. An unstable model is usually characterized by a non-zero value, often fluctuating; the maximum unbalanced force and increased displacements (Eberhardt, 2003). Also, areas of low stresses are favorable to the internal erosion (Ormann et al., 2010).

2.3 Geophysical analysis by computed tomography

The computed images of the electrical tomography using a freeware (RES2DINV software) can be interpreted as an electrical conductivity map showing that the conductive areas through the embankment are correlated with water saturated areas where electrical resistivity values are low in favor of a high conductivity.

3. RESULTS

3.1 Embankment stability analysis using SLOPE/W

The input parameters for each type of material are: unit weight (γ), effective cohesion (c’) and effective internal angle of friction φ’ (cf. Table 1).

Figure 3 shows the result of the analysis that indicates a factor of safety (FS) value of 1.833 which is higher than the recommended value of FS = 1.5. This value corresponds to the start of the tailings impoundment filling which is the current state of the embankment. This result shows that the embankment is currently stable (Figure 3). When 10 tons static dead-weight is applied on the crest of the embankment, simulating a stationary truck during waste rock damping, the factor of safety remains above 1.5 but decreases to 1.754. When the tailings impoundment is entirely filled the factor of safety decreases slightly from 1.833 to 1.814.

To determine the effects of the change in cohesion and the angle of friction of fill layers (rockfill and tailings), several simulations were performed and the values the factors of safety are shown in Table 2. One can observe that there would be embankment failure when the tailings effective cohesion *c’* is zero and the effective internal angle of friction is 12° (FS = 0.755). Also, when the tailings effective cohesion is zero with an angle of friction of 35° and a unit weight of 12 kN/m^3, the factor of safety FS = 1.28 (which is lower than the recommended value of 1.5).

It should however be noted that these two scenarios are unlikely because the tailings effective angle of friction would be close to 30° while it is very unlikely that the tailings can have a unit weight lower than 14 kN/m^3 (specific gravity of 2.67 and slurry solid mass content of 50%).

Table 1: Values of parameters used in SLOPE/W simulations (from the report of the closure plan and restoration, 1999).

Type of material	Unit weight (kN/m³)	Angle of friction (°)	Cohesion (kPa)	Undrained shear strength (kPa)
Tailings	19.0	35	0	0
Upper silt	19.2	28	0	0
Lower silt	19.2	28	0	0
Silty clay	16.5	30	0	40
Rockfill	20	42	0	46
Filling material	19	35	0	0

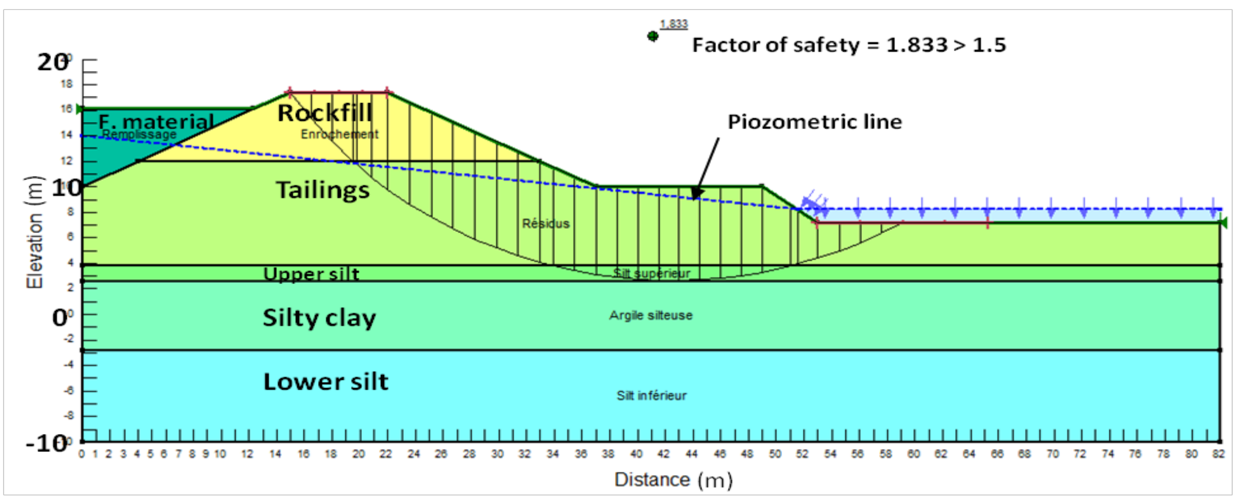

Figure 3: Stability analysis of the embankment slope showing a FS of 1.833 at the start of the tailings impoundment filling.

Data in Table 2 are used to construct different graphs that are presented in Figures 4, 5, and 6 and illustrate the influence of the effective cohesion and internal angle of friction on the factor of safety. These figures show that the effective cohesion and angle of friction (which are the shear strength parameters shown in Eq. 3) have a direct influence on the factor of safety. In fact, FS increases with the increase of the cohesion and the angle of friction. For a similar range of variation of *c*’ and φ’ the trend of the factor of safety is more pronounced for the tailings than for the rockfill (Figure 6).

Table 2: Factor of safety when we vary the cohesion and the angle of friction of rockfill and tailings layers independently.

Type of material	Cohesion (kPa)	Angle of friction (°)	Unit weight (kN/m³)	Factor of safety
Rockfill	0	20	18.1	1.856
	0	42	18.1	1.964
	0	60	18.1	2.072
	0	42	18.1	1.964
	10	42	18.1	2.013
	20	42	18.1	2.064
	0	42	18.1	1.964
	0	42	23.1	1.848
	0	42	24.3	1.824
	0	42	30	1.729
Tailings	0	12	19	0.755
	0	35	19	1.964
	0	53	19	2.582
	0	35	19	1.964
	10	35	19	2.222
	20	35	19	2.391
	0	35	12	1.28
	0	35	19	1.964
	0	35	25	2.349

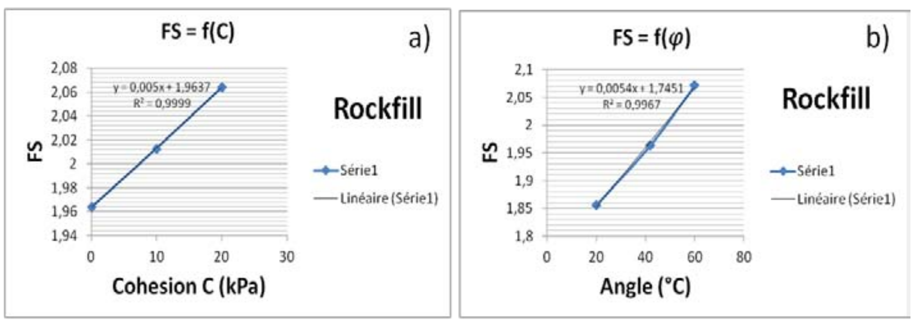

Figure 4: Variation in the factor of safety as a function of a) the cohesion and b) the angle of friction of the rockfill layer.

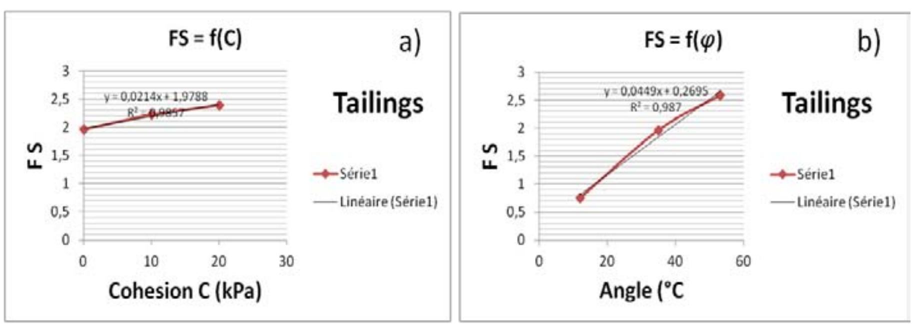

Figure 5: Variation in the factor of safety as a function of a) the cohesion and b) the angle of friction of the tailings layer.

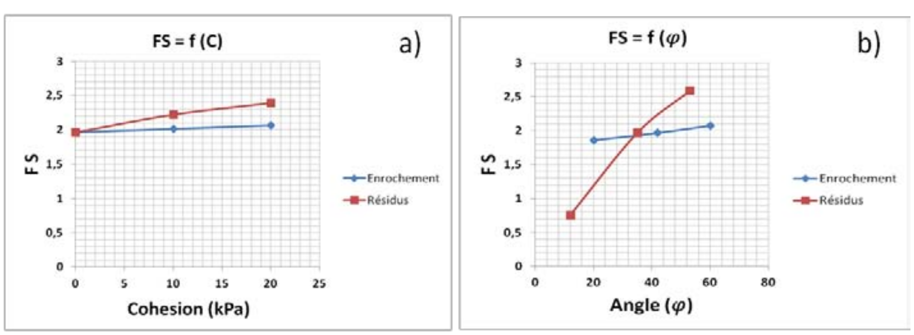

Figure 6: Variation in the FS as a function of a) effective cohesion and b) internal angle of friction for rockfill and tailings.

3.2 Stress-strain analysis using SIGMA/W

The input parameters to perform the stress-strain analysis of the embankment using the SIGMA/W code are listed in Table 3. The values are representative of each material in the embankment. The stress analysis shows that if the pore water pressure does not dissipate easily in short term, the total stress could increase progressively and put the embankment stability in question. The pore water pressure was relatively high in the deeper layers, particularly in the regions directly below the embankment (i.e. below the rockfill and tailings) and moving toward the downstream side (Figure 7).

Table 3: Values of parameters used in SIGMA/W.

Parameters	Rockfill	Tailings	Upper silt	Silty clay	Lower silt	Filling material
Young's Modulus E (kPa)	40000	7200	3895	9312	9800	3048
Unit Weight (kN/m³)	24.3	19	19.2	16.5	19.2	19
Poisson's ratio	0.334	0.334	0.334	0.334	0.334	0.334
In situ pressure coefficient K_0	0.5001	0.5001	0.5001	0.5001	0.5001	0.5001

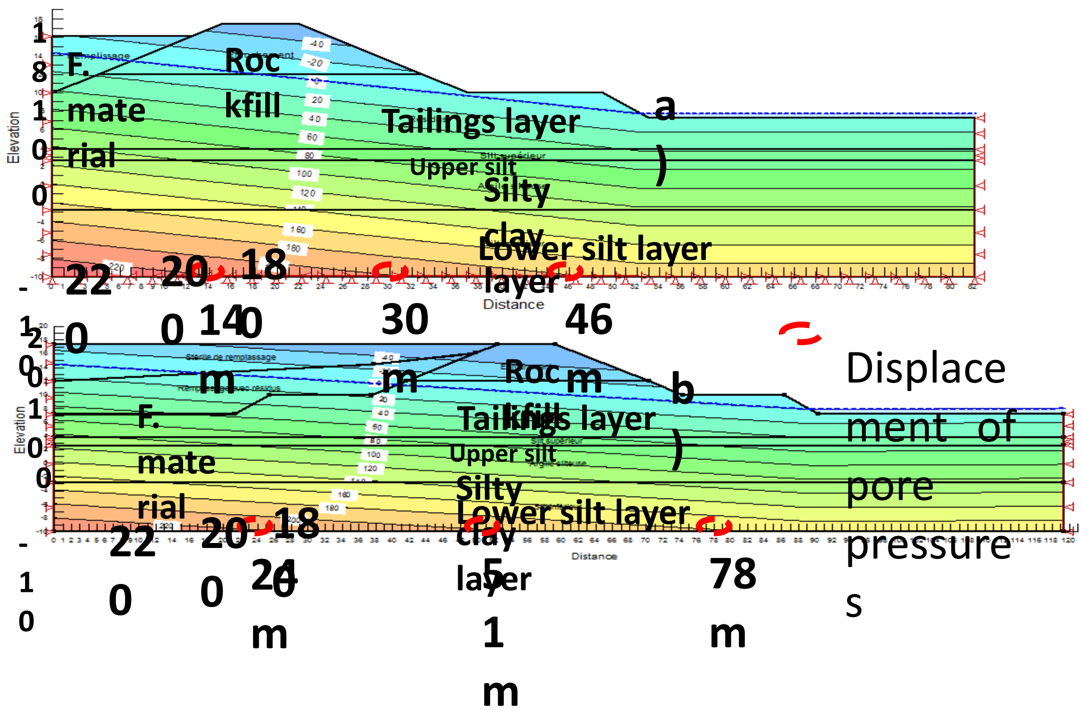

Figure 7: Illustration of the iso-value curves of pore pressure for a) current in-situ condition, b) filled state.

3.3 Geophysical tomography using RES2DINV software

The geophysical method used was the electrical resistivity method in which an electric current is injected into the embankment using different electrodes placed at different locations, and then the potential difference between a pair of potential electrodes is measured. The apparatus used was the ground penetrating radar (GPR). According to the system set up, a section of the apparent resistivity was be calculated from the potential measurements. Two measurement configurations were used: Wenner and Wenner-Shlumberger (Syscal R1 Plus Switch 72) in order to look at the variation of the resistivity within the embankment related to its internal structure. Figure 8 shows an inversion result from data collected with Wenner-Schlumberger configuration using the RES2DINV software. In this figure the blue color represents the low resistivity (i.e. high conductivity) and the red color represents the high resistivity. The distribution of the apparent resistivity outlines a layered structure of the embankment. An outcrop (observed in the field) at the end of the profile on the right (at around 320 m) corresponds to the highest resistivity area (dark brown to purple). The resistivity variation with the depth correlates very well with the internal structure observed from the geotechnical drilling F-95-1 observations performed by Golder and Associates in 1996; especially at the depth of the interface between the moraine and the bedrock. Based on the drilling data, the following lithological limits from top to bottom on the sections in Figure 8 were identified:

The rockfill layer (0 – 5 m approximately), with electrical resistivity of between 65 and 117 Ωm;

Tailings layer (5 – 26 m approximately), electrical resistivity between 20 and 65 Ωm;

Upper silt, silty clay, lower silt, dense moraine and bedrock (> 26 m of depth), electrical resistivity between 117 and 1222 Ωm;

The bedrock is located in sub-surface to the right end of the section and it might have the same composition as that on the bottom of the embankment. Lateral variations in resistivity may imply that there are resistivity heterogeneities within the embankment in particular between the moraine and the sub-surface rock (lowest resistivity area). These heterogeneities may be due to cracks filled with water (dark blue);

In the pond (downstream of the dam), it seems that there is a penetration of tailings drainage water through the dam. It could be caused by small cracks where there is a discontinuity of resistivity (red dashed cycle on Figure 8) of the embankment layers materialized by resistivity variations.

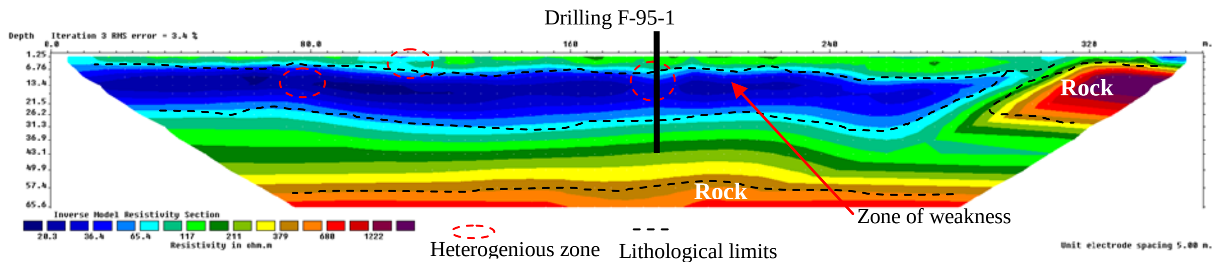

Figure 8: Tomographic inversion image, Wenner-Schlumberger with 5m distance between electrodes.

4. CONCLUSION

Stability analysis performed was particularly interesting as a monitoring tool for the Westwood Mine embankment. The calculated values of the factor of safety were higher than 1.5, which meets the standard recommendations set by some authors and by the Quebec Ministry of Natural Resources and Wildlife for static loading and steady flow conditions. In all cases of realistic geometric representation of the embankment, the minimum factor of safety was greater than 1.5, thus confirming the stability of the embankment studied. The stress analysis suggests that the pore water pressure is higher in the layers directly below the embankment (i.e. higher in the upper silt, silty clay and lower silt). The performed electrical tomography shows that it is possible to distinguish the different structures of the Northwest embankment of Westwood Mine tailings storage facility without employing a destructive method. The electrical tomography image shows that the conductive areas across the embankment correlate well with water saturated areas such as tailings layer where electrical resistivity values are low in favor of a high conductivity. These water-saturated areas are susceptible to the risk of internal erosion. The change in electrical resistivity scale in the rockfill layer (5 m depth) shows that it is unsaturated layer having a lower electrical resistivity (approximately 65 – 117 Ωm). These zones could reflect heterogeneity of the particle size of these materials, which could cause differential settlement in the long term.

5. ACKNOWLEDGEMENT

This research was financially supported by the RIME (Research Institute of Mining and Environment) of UQAT. The authors would like to acknowledge them for this support. The authors also wish to thank our mining partner, IAMGOLD Corporation (Westwood Mine), including the Superintendent of Environment Department, Mr. Sylvain Lortie for their collaboration in this project.

6. REFERENCES

Barbour, S. L., and Krahn, J. (2004). Numerical modelling – prediction or process? Geotechnical news, December 2004.

Denahan B. J., Smith D. L., (1984). Electrical resistivity investigation of potential cavities underlying a proposed ash disposal area. Environmental geology and water sciences. Volume 6, Issue 1, pp 45-49.

Eberhardt, E. (2003). Rock slope stability analysis - Utilization of advanced numerical techniques.

Ernstson, K., Kirsch, R., (2006). Geoelectrical methods. In: Kirsch, Reinhard (Ed.), groundwater geophysics. Springer. ISBN: 3-540-29383-3, pp. 85–117.

GEO-SLOPE International Ltd. (2007). Geo-Slope Office (Slope/W, Seep/W, Sigma/W, CTran/W, Temp/W, Quake/W, Air/W). Geo-Slope International Ltd., Calgary, Canada.

Mériaux P., Royet P., Folton C. (2001). Surveillance, entretien et diagnostic des digues de protection contre les inondations. Cemagref Editions, 191 p.

Ormann, L., Zardari, M.A., Mattsson, H., Bjelkevik, A., and Knutsson, S., (2010). Numerical analysis of strengthening by rockfill embankments on an upstream tailings dam.